

AN INNER GASEOUS DISK AROUND THE HERBIG BE STAR MWC 147

T. BAGNOLI¹, R. VAN LIESHOUT¹, L. B. F. M. WATERS^{1,2}, G. VAN DER PLAS¹, B. ACKE², H. VAN WINCKEL², G. RASKIN²,
P. D. MEERBURG^{1,3}

¹ Astronomical Institute “Anton Pannekoek”, University of Amsterdam, Science Park 904, 1098 XH Amsterdam, The Netherlands

² Instituut voor Sterrenkunde, K.U. Leuven, Celestijnenlaan 200 D, 3001 Leuven, Belgium and

³ Institute for Theoretical Physics, University of Amsterdam, Valckeniersstraat 65, 1018 XE Amsterdam, The Netherlands

Draft version October 8, 2010

ABSTRACT

We present high-spectral-resolution, optical spectra of the Herbig Be star MWC 147, in which we spectrally resolve several emission lines, including the [O I] lines at 6300 and 6363 Å. Their highly symmetric, double-peaked line profiles indicate that the emission originates in a rotating circumstellar disk. We deconvolve the Doppler-broadened [O I] emission lines to obtain a measure of emission as a function of distance from the central star. The resulting radial surface brightness profiles are in agreement with a disk structure consisting of a flat, inner, gaseous disk and a flared, outer, dust disk. The transition between these components at 2 to 3 AU corresponds to the estimated dust sublimation radius. The width of the double-peaked Mg II line at 4481 Å suggests that the inner disk extends to at least 0.10 AU, close to the corotation radius.

Subject headings: circumstellar matter — stars: emission-line, Be — stars: individual (MWC 147) — stars: pre-main sequence — stars: variables: T Tauri, Herbig Ae/Be — protoplanetary disks

1. INTRODUCTION

Herbig Ae/Be (HAeBe) stars are intermediate-mass ($2 - 8 M_{\odot}$), pre-main sequence stars, known to be surrounded by circumstellar disks of gas and dust where planets may form (see e.g. Waters & Waelkens 1998; Natta et al. 2000). The details of the disk structure, especially the innermost region ($R \lesssim 1$ AU), are still a matter of debate.

For about a decade, near-infrared (NIR) interferometers have been able to resolve the disk at ~ 1 AU scales. These NIR interferometric observations, together with NIR spectral energy distribution (SED) modeling, have led to disk models for HAe and late type HBe stars, featuring an optically-thin inner hole and a “puffed-up” inner dust wall at the dust sublimation radius (Millan-Gabet et al. 2007, and references therein). The interferometric observations of some early type HBe stars, however, cannot be explained by this model, and the nature of their inner disks is still unclear. In a broader context, the HBe stars form a transition between lower mass T Tauri and HAe stars, and more massive young stellar objects. Fundamental processes in disk structure and evolution, such as grain growth, disk dissipation, and possibly planet formation, may change in the mid-B spectral range. This is probably related to the effects of shorter evolutionary timescales and stronger stellar radiation fields (e.g. Gorti & Hollenbach 2009). An interesting object in the transitional regime is MWC 147 (alias HD 259431).

MWC 147 was classified as a B6 type star by Hernández et al. (2004). They estimate its mass at $6.6 M_{\odot}$ and age at 3.2×10^5 yr, assuming a distance of 800 pc and $R_V = 3.1$. Compared to other HAeBe stars, MWC 147 seems to have a relatively high mass accretion rate ($4.1 \times 10^{-7} M_{\odot} \text{ yr}^{-1}$ Brittain et al. 2007; $7 \times 10^{-6} M_{\odot} \text{ yr}^{-1}$ Kraus et al. 2008). There is also

evidence for a strong stellar wind (Bouret et al. 2003), with an associated mass loss rate of $\sim 10^{-7} M_{\odot} \text{ yr}^{-1}$ (Skinner et al. 1993; Nisini et al. 1995). Several studies (Polomski et al. 2002; Bouret et al. 2003) find evidence for a flaring circumstellar disk around the object. Recently, Kraus et al. (2008) proposed a disk structure composed of an outer, flared, irradiated dust disk and an inner, optically thick, gaseous accretion disk. They find that the disk should be notably inclined ($i \approx 40^{\circ} - 60^{\circ}$).

In this paper, we present a description and analysis of various emission lines in the optical spectrum of MWC 147, resolved at very high spectral resolution. Emission features can be used to probe the gas component of the circumstellar environment of HAeBe stars, carrying information about its structure and dynamics. Section 2 introduces our observations and explains how the data were reduced. In Section 3, we describe the most prominent spectral features and apply a method developed by Acke et al. (2005) and Acke & van den Ancker (2006) to resolve a rotating circumstellar disk from forbidden oxygen lines. Finally, in Section 4, we discuss our results in the light of previous research and draw conclusions about the nature of the disk around MWC 147.

2. OBSERVATIONS AND DATA REDUCTION

We obtained two echelle spectra of MWC 147 using the HERMES spectrograph (Raskin & van Winckel 2008) mounted on the 1.2 m Mercator telescope, located at La Palma, Spain. The instrument covers the full optical wavelength range from 3770 to 9000 Å with a spectral resolution of $\lambda/\Delta\lambda \approx 85000$ in High Resolution Mode. The observations (45 minutes exposures) were performed on 2009 October 14 and 19, and the resulting spectra have signal-to-noise ratios (S/N; determined around 6300 Å) of about 170 and 140 respectively. The HERMES pipeline was used for initial data reduction, including order extraction, background subtraction, flat-

TABLE 1
QUANTITATIVE PROPERTIES OF THE EMISSION LINES SHOWN IN
FIGURE 1.

Line	EW [Å]	$FWHM$ [km s ⁻¹]	$FW.1M$ [km s ⁻¹]
[O I] 6300 Å	-0.564 ± 0.003	39	64
[O I] 6363 Å	-0.173 ± 0.003	39	61
[O I] 5577 Å	-0.044 ± 0.001	51	89
O I 8446 Å	-5.300 ± 0.047	106	201
Mg I 8807 Å	-0.422 ± 0.011	190	302
Mg II 4481 Å	-0.019 ± 0.015	312	378
H α	-63.202 ± 0.099	190	422

field correction, and wavelength calibration.

Further data reduction was performed using IRAF. For most of our analysis we used the average-combined spectrum of both observations to achieve a higher S/N of about 220. After determining the continuum using standard IRAF routines, the spectra were normalized to unity. Telluric absorption lines and [O I] emission from Earth's atmosphere were removed by fitting and subtracting a Gaussian. Spectral regions polluted by cosmic rays were cut out.

We determined the radial velocity of MWC 147 by comparing the observed and theoretical line centers of two photospheric He I absorption lines at 4471 and 5876 Å. Line centers were measured by fitting Gaussians to the line profiles, and an error was calculated from the variance of several measurements each using a different continuum estimate. We find a heliocentric radial velocity of 21.4 ± 0.3 km s⁻¹, which is consistent with cataloged values (19.00 ± 4.1 km s⁻¹ Barbier-Brossat & Figon 2000; 23 ± 2 km s⁻¹ Vieira & Cunha 1994). The spectra shown in this paper were converted to velocity space and centered on the photospheric velocity of the star.

3. ANALYSIS

3.1. The optical spectrum of MWC 147

The spectrum of MWC 147 contains numerous emission lines, including both permitted and forbidden transitions of various elements, many of which are double-peaked. The emission lines most relevant to our analysis ([O I] 6300, 6363, 5577 Å, O I 8446 Å, Mg I 8807 Å, Mg II 4481 Å and H α) are shown in Figure 1. For these lines we determined the equivalent width (EW), full width at half maximum ($FWHM$) and full width at 10% of maximum intensity ($FW.1M$). An error on the EW s is calculated from the variance of several measurements using different continuum estimates. The resulting values are presented in Table 1. For the [O I] 6300 Å line we furthermore assessed the degree of symmetry by drawing its bisector (see Figure 2). Note that the [O I] 5577 Å line is usually undetected in H AeBe stars, a relevant point for determining the origin of the [O I] emission (see Section 3.2).

The emission lines shown in Figure 1 all feature double-peaked, extremely symmetric profiles, except Mg II 4481 Å, in which the core of the emission is affected by photospheric absorption. These line profiles strongly suggest the presence of a circumstellar disk in Keplerian rotation. The [O I] 6300 Å line consists of two compo-

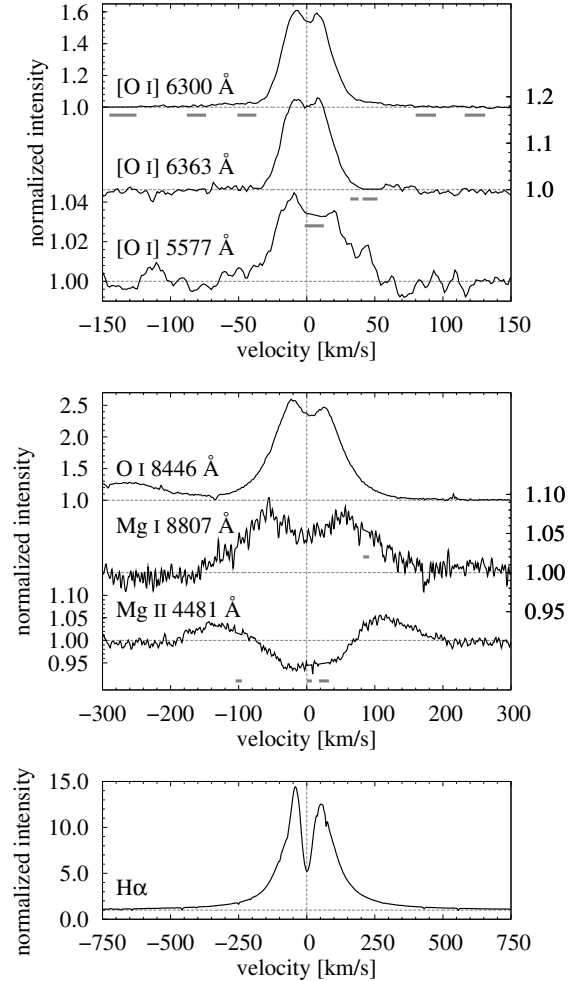


FIG. 1.— Line profiles of several emission lines in the MWC 147 spectrum. The lines are centered on the stellar radial velocity, indicated by the vertical dotted line. The continuum is shown by horizontal dotted lines. The location of the telluric features and cosmic rays that were removed is indicated by thick horizontal bars. For the [O I] 5577 Å line only the observation of 19 October was used, since the other observation was severely polluted. The spectrum of the [O I] 5577 Å line was smoothed using a 5-point boxcar average. The O I 8446 Å line is blended with P18 in the blue wing. Note the different intensity and velocity scales.

nents. The bulk of its emission is found at low velocities (less than about 35 km s⁻¹), while weak wings extend up to at least 70 km s⁻¹. This morphology is examined in more detail in Section 3.3.

If the emission lines emanate from a circumstellar disk, the line width is dominated by rotation and indicates at what radial distance from the star the emission originates. In this scenario, the narrow forbidden lines are created furthest away from the star where gas densities are sufficiently low, followed by the broader permitted lines of neutral species closer to the star. The ionized Mg line emanates from the region closest to the star, consistent with the higher temperature required for the ionization.

Assuming a stellar mass of $6.6 M_{\odot}$ and a Keplerian rotating disk with an inclination of 50° , the $FW.1M$ of the Mg II 4481 Å line corresponds to an inner radius of the emission region of about 0.10 AU. This is quite close to the corotation radius (where the Keplerian rotating

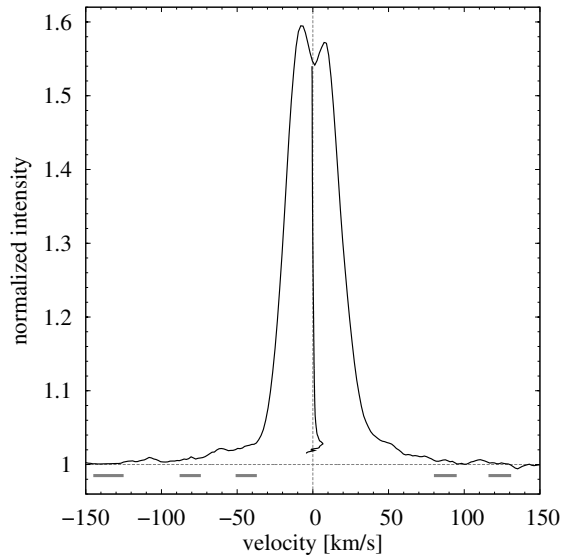


FIG. 2.— The [O I] 6300 Å line with its bisector. The spectrum was smoothed using a 5-point boxcar average to suppress noise, allowing the bisector to be drawn further down. The horizontal dotted line indicates the continuum level, the vertical dotted line the stellar radial velocity. Removed telluric absorption lines and cosmic rays are indicated by thick horizontal bars. Note the high degree of symmetry of the line.

disk has the same angular velocity as the rigidly rotating star) of approximately 0.07 AU, found using a stellar rotational velocity corresponding to $v \sin i = 90 \text{ km s}^{-1}$ (Böhm & Catala 1995), and a stellar radius of $6.6 R_{\odot}$, calculated from the luminosity and effective temperature estimates of Hernández et al. (2004). The $H\alpha$ line may be broadened significantly by electron scattering and should therefore not be analyzed in this way.

3.2. Origin of [O I] emission

Störzer & Hollenbach (2000) identified two mechanisms that contribute to [O I] emission in photodissociation regions. In high temperature environments ($T > 3000 \text{ K}$), oxygen atoms can be thermally excited due to collisions with hydrogen atoms and free electrons. Alternatively, the excited oxygen atoms can be the result of photodissociation of OH molecules by ultraviolet (UV) radiation.

[O I] emission in HAeBe stars was studied in detail by Acke et al. (2005). Based on the non-detection of the [O I] 5577 Å line in all sample stars with coverage at this wavelength, they derive an upper excitation temperature (T_{exc}) limit from the upper limit on the 6300 Å to 5577 Å line flux (LF) ratio, assuming the emission is fully thermal. Since the resulting T_{exc} limit is lower than 3000 K, they exclude the thermal channel, and propose that the UV radiation from the star provides all the excited oxygen atoms.

In the case of MWC 147, however, the observed $LF(6300)/LF(5577)$ ratio of about 10 corresponds to a T_{exc} of 4000 to 5000 K, assuming the [O I] emission is fully thermal. Therefore, we cannot exclude that thermally excited atoms contribute to the emission. The reason for this may be the higher luminosity and temperature of MWC 147.

3.3. The [O I] surface brightness profile

We use the [O I] lines at 6300 and 6363 Å to derive the spatial distribution of the O I atoms in the disk. These emission lines are well suited for this purpose, because they probe the (irradiated) disk surface, are optically thin, and do not suffer from underlying photospheric absorption. Their spectral shape is a consequence of the velocity field of the emitting region. By assuming the velocity field to be Keplerian and providing a stellar mass and disk inclination, it is possible to derive the spatial distribution of [O I] emission from the line profiles. First, the red and blue wing of the line are averaged. Then, the highest-velocity bin that contains [O I] flux is attributed to the innermost ring of the disk, which rotates the fastest. Due to projection effects, this ring adds emission to the whole line profile. Its theoretical contribution is computed and removed, and the procedure is iterated on the residuals of the line from the extrema inwards, until the whole line profile is dismantled to its very core at $v = 0$. This *spectral deconvolution* method, based on the model for [O I] emission in HAeBe stars of Acke et al. (2005), is explained in more detail by Acke & van den Ancker (2006, their Section 4.2), and applied to three more stars by van der Plas et al. (2008).

We compute radial surface brightness profiles from the [O I] lines at 6300 and 6363 Å, adopting a stellar mass of $6.6 M_{\odot}$ and disk inclination of 50° (see Figure 3). The most striking result is the clear dichotomy in the profile derived from the 6300 Å line. It features a shallow plateau from roughly 1 to 2.5 AU (corresponding to the high velocity wings of the emission line), and a much stronger component from about 2.5 AU outwards, peaking around 20 AU (corresponding to the core of the line). The dependence of these values on disk inclination is relatively weak, with the division between the two components varying between 2 and 3 AU for inclinations between 40° and 60° respectively. The profile derived from the 6363 Å line has a very similar behavior, but does not show an inner component. This can be explained by the intrinsic weakness of the 6363 Å line (the ratio of the Einstein transition rates of the lines is $A_{6300}/A_{6363} = 3.0$), and the slightly lower S/N achieved in this part of the spectrum, which would blend any possible high velocity wings into the noise of the continuum.

The observed distribution of emitting atomic oxygen as a function of radius can be explained by a disk model consisting of a weakly emitting inner disk and a strongly emitting outer disk. The transition between these two components lies between approximately 2 and 3 AU. The outer radius of the emission region cannot be derived accurately from the line profile, since Keplerian rotational velocity goes to zero at large distances from the star. Nonetheless, [O I] emission is present up to at least 100 AU from the star. At this distance, our spectral resolution is still sufficient to resolve the disk kinematics.

4. DISCUSSION AND CONCLUSIONS

We have presented optical spectra of MWC 147, featuring various double-peaked emission lines. The observed differences in line width are consistent with a highly stratified circumstellar structure in which line shape is dominated by rotation. The double-peaked emission

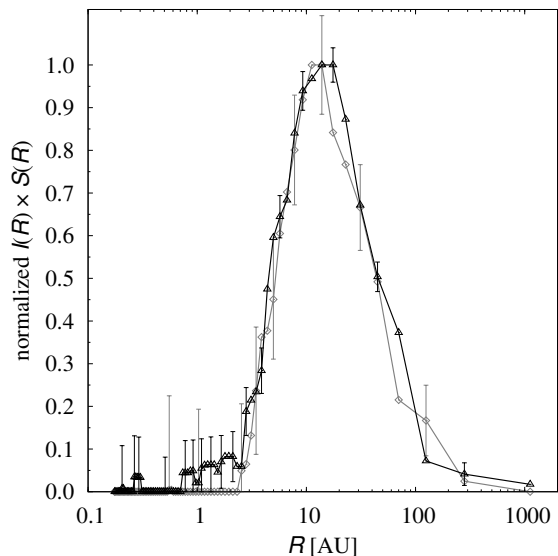


FIG. 3.— The intensity versus radius graphs $I(R)$ derived from the line profiles of the [O I] 6300 (black, triangles) and 6363 Å (gray, diamonds) emission lines. Intensities have been multiplied by surface $S(R)$ of a ring of the disk at distance R and normalized to peak intensity. Error bars, derived from the S/N of the spectra, are shown every third data point. A distinct inner and outer disk component can clearly be seen in the data derived from the [O I] 6300 Å line. The boundary of these components corresponds to the estimated dust sublimation radius. The inner component is not seen in the weaker 6363 Å line.

lines are highly symmetric and centered on the stellar radial velocity derived from He I absorption lines. These properties indicate emission from the surface of a rotating, circumstellar disk. The observation of Mg II emission close to the corotation radius shows that this disk extends to very close to the stellar surface.

According to Acke et al. (2005), [O I] emission in HAeBe stars cannot be due to thermal excitation. They suggest that photodissociation of OH molecules by UV radiation from the star provides the excited neutral oxygen atoms. The 6300 Å to 5577 Å line flux ratio of about 10 observed in MWC 147 is in agreement with values predicted by Störzer & Hollenbach (2000) for this nonthermal excitation mechanism in photodissociation regions. However, we cannot exclude a thermal contribution to the lines for MWC 147, which has a much higher luminosity than most of the stars discussed by Acke et al. (2005).

Analysis of the [O I] 6300 Å line shows that the disk is composed of a weakly emitting inner component and a more strongly emitting outer part, with the break between the two components at 2 to 3 AU. This matches the dust sublimation radius estimate of 2.7 AU by Kraus et al. (2007, 2008, assuming a dust sublimation temperature of 1500 K), in the framework of their disk model composed of a flat inner gaseous disk and a flaring outer dust disk. The change in disk geometry at the dust sublimation radius is likely to cause a steep density gradient in the upper disk atmosphere, due to the strong change in disk scale height, related to the decreased opacity of the inner disk. If the hydrogen density rises above the critical value of $6 \times 10^9 \text{ cm}^{-3}$ (Störzer & Hollenbach 2000), collisional de-excitation hampers the radiative channel, resulting in

a (much) weaker [O I] emission. Densities around this critical value are plausible for the inner regions of protoplanetary disks surrounding intermediate-mass pre-main sequence stars (van der Plas et al., in preparation, based on Woitke et al. 2009). Detailed modeling is needed to establish this connection quantitatively. We note that the permitted O I 8446 Å line is much broader than the forbidden lines (Figure 1) and does not show a break at the velocity corresponding to the estimated dust sublimation radius. This excludes a drastic change in the O I abundance as an explanation for the observed two-component [O I] 6300 Å line profile. Furthermore, in a larger sample of HAe stars the inner radius of the [O I] emitting region derived from the [O I] line shape is similar to that of the dust sublimation radius (van der Plas, private communication), as is the case for the strong component of the [O I] emission in MWC 147. Whether or not the inner disk in MWC 147 is an accretion disk as Kraus et al. (2008) suggest is unclear.

It is interesting to compare the geometry of the disk of MWC 147 to those of less luminous HAeBe stars. There is growing evidence from interferometric studies that the lower mass HAe stars have material inside the dust sublimation radius (e.g. Benisty et al. 2010) whose nature is not well constrained. Both gas and refractory dust have been proposed. The higher luminosity of MWC 147 forces the dust sublimation radius to larger distance, allowing the inner regions to appear more pronounced in imaging and spectroscopy. The case of MWC 147 clearly proves that an innermost gaseous disk is possible.

Analysis of the infrared SED of MWC 147 by Verhoeff et al. (2010) suggests either a self-shadowed disk or a disk with a small but not well constrained outer radius. These authors show that emission from Polycyclic Aromatic Hydrocarbons (PAHs) detected in a Spitzer IRS spectrum arises from the environment and is weak or absent in the disk. This implies that MWC 147 does not follow the trend that strong emission in [O I] 6300 Å is usually seen in disks with strong PAH emission (Acke et al. 2005). Strong emission in these gas tracers is usually interpreted as evidence for a flaring disk. If the presence of [O I] 6300 Å emission up to distances of ~ 100 AU is due to non-thermally excited O I, then a gaseous flaring disk must be present extending to these distances. This would favor a scenario in which PAHs are destroyed by the strong UV radiation field of the star.

The age of the disk (3.2×10^5 yr, Hernández et al. 2004) is comparable to the expected evaporation timescale for a $6 - 7 M_{\odot}$ star ($\sim 10^5$ yr, Gorti & Hollenbach 2009). It is therefore expected to be in a phase of significant evaporation. Our observations constrain the disk to extend to at least 100 AU, suggesting that at this distance it has not yet significantly been eroded by the stellar radiation field.

We would like to thank the anonymous referee for a careful review of the letter. This study is based on observations made with the Mercator Telescope, operated on the island of La Palma by the Flemish Community, at the Spanish Observatorio del Roque de los Muchachos of the Instituto de Astrofísica de Canarias.

The HERMES project is a collaboration of the K.U.Leuven, ULB and ROB of Belgium with smaller

contributions from the Tautenburg Landessterwarte and the Geneva observatory. The Hermes team acknowledges support from the Fund for Scientific Research of Flanders

(FWO), from the Research Council of K.U.Leuven, from the Fonds National Recherches Scientific and from the Royal Observatory of Belgium.

Facilities: Mercator1.2m (HERMES).

REFERENCES

- Acke, B., & van den Ancker, M.E. 2006, A&A, 449, 267
 Acke, B., van den Ancker, M.E., & Dullemond, C.P. 2005, A&A, 436, 209
 Barbier-Brossat, M., & Figon, M. 2000, A&AS, 142, 217
 Benisty, M. et al. 2010, A&A, 511, 74
 Böhm, T., & Catala, C. 1995, A&A, 301, 155
 Bouret, J.-C., Martin, C., Deleuil, M., Simon, T., & Catala, C. 2003, A&A, 410, 175
 Brittain, S. D., Simon, T., Najita, J. R., & Rettig, T. W. 2007, ApJ, 659, 685
 Gorti, U. & Hollenbach, D. 2009, ApJ, 690, 1539
 Hernández, J., Calvet, N., Briceño, C., Hartmann, L., & Berlind, P. 2004, AJ, 127, 1682
 Kraus, S., Preibisch, T., & Ohnaka, K. 2007, in Proceedings IAU Symposium No. 243, Star-Disk Interaction in Young Stars, ed. J. Bouvier & I. Appenzeller (Cambridge: CUP), 337
 Kraus, S., Preibisch, T., & Ohnaka, K. 2008, ApJ, 676, 490
 Millan-Gabet, R., Malbet, F., Akeson, R., Leinert, C., Monnier, J., & Waters, R. 2007, in Protostars & Planets V, ed. B. Reipurth, D. Jewitt, & K. Keil (Tucson: University of Arizona Press), 539
 Natta, A., Grinin, V., & Mannings, V. 2000, in Protostars & Planets IV, ed. V. Mannings, A. P. Boss, S. S. Russell (Tucson: University of Arizona Press), 559
 Nisini, B., Milillo, A., Saraceno, P., & Vitali, F. 1995, A&A, 302, 169
 Polomski, E. F., Telesco, C. M., Piña, R., & Schulz, B. 2002, AJ, 124, 2207
 Raskin, G., & van Winckel, H. 2008, Proc. SPIE, Vol. 7014, 70145D
 Skinner, S. L., Brown, A., & Stewart, R. T. 1993, ApJS, 87, 217
 Störzer, H., & Hollenbach, D., 2000, ApJ, 539, 751
 van der Plas, G., van den Ancker, M. E., Fedele, D., Acke, B., Dominik, C., Waters, L. B. F. M., & Bouwman, J. 2008, A&A, 485, 487
 Verhoeff et al. 2010, A&A, in press
 Vieira, S. L. A., & Cunha, N. C. S., 1994, Inf. Bull. Variable Stars, 4090, 1
 Waters, L. B. F. M., & Waelkens, C. 1998, Ann. Rev. Astron. Astrophys., 36, 233
 Woitke, P., Kamp, I., & Thi, W.-F. 2009, A&A, 501, 383